Journal of Low Temperature Physics, Vol. 137, Nos. 1/2, October 2004 (© 2004)

Repulsive Flux Pinning Force in NbTi/Nb Superconductor/Superconductor Multilayers

Y. Obi,[1] M. Ikebe,[2] and H. Fujishiro[2]

[1] *Institute for Materials Research, Tohoku University, 2-1-1 Katahira, Aobaku, Sendai 980-8577, Japan*
E-mail: obi@imr.tohoku.ac.jp
[2] *Faculty of Engineering, Iwate University, 4-3-5 Ueda, Morioka 020-8551, Japan*

(Received December 8, 2003; revised May 14, 2004)

Flux pinning characteristics have been investigated for the $Nb_x\ Ti_{100-x}/Nb$ ($x = 65$, 50 and 28) and $Nb_{28}Ti_{72}/Nb_{65}Ti_{35}$ superconductor(S)/superconductor(S′) multilayers. The maximum of the pinning force $F_{p\perp max}$ perpendicular to the layer plane as a function of the structure modulation length λ has a peak in the quasi-two-dimensional region ($\lambda \sim 20$ nm). The maximum. values of the $F_{p\perp max}$ versus λ curve are proportional to the difference of the GL coherence length (ξ_{GL}) between the superconductive sublayers S and S′. The results suggest that the large $F_{p\perp max}$ in the S/S′ multilayer is caused by the repulsive pinning force due to Nb layers with larger ξ_{GL}.

KEY WORDS: superconductivity; critical current; pinning force; multiplayer.

1. INTRODUCTION

The study of the mechanism of flux pinning is one of the most attractive subjects for superconducting multilayers because the superconducting multilayer is considered to have intrinsic large pinning centers due to the intervening normal or superconducting layers with different superconducting characteristics. There have been several theoretical and experimental investigations concerning the subject of the pinning mechanism for superconducting multilayers.[1–5] Much of recent theories have been concentrated on the high T_c oxide superconductors. Some of these theories can be applicable to the multilayered materials with a certain modification because oxide superconductors have a layered structure composed of the strongly superconductive Cu–O layer and weakly superconductive other layers. One

0022-2291/04/1000-0125/0

of typical theories applicable to the transverse pinning force for multilayers is the conception of the intrinsic pinning force introduced by Tachiki and Takahashi.[6] This idea is based on the fact that the layered structure itself should play an important role for flux pinning due to the oscillative spatial variation of the order parameter perpendicular to the periodic layered structure; the weak superconducting layer should stabilize the flux located in these layers.

Experimentally there have been several studies of the critical current density J_c and the pinning force F_p for the multilayers. For example, Raffy and Renard[7] have observed the peak effect in J_c versus H curves for Pb/Bi superconducting multilayers. They interpreted the peak effect as a result of the geometrical matching between the distance of the fluxoids and the distance of the pinning centers. Brossard and Geballe[8] investigated the longitudinal $F_{p\parallel}$ and transverse $F_{p\perp}$ pinning force, which act parallel and perpendicular to the layer plane, respectively, for the Nb/Ta multilayers. Estimating the reduced pinning force F_p/F_{pmax} as a function of reduced magnetic field H/H_{c2}, they concluded that for large bilayer period the pinning force behaves as a dislocation pinning and for small bilayer period it originates from the collective pinning mechanism. We have investigated the pinning mechanism for Nb/Al_2O_3 multilayers,[9,10] and shown that for the longitudinal pinning force $F_{p\parallel}$ the surface pin plays an important role. We also have investigated the transverse pinning force $F_{p\perp}$ for Nb/Ti multilayers.[11] In this case the large enhancement of $F_{p\perp}$ as a function λ was observed for the quasi 2D-region. But until now the exact mechanism of the transverse pinning for multilayers has not been clarified yet. Recently, we have investigated the pinning mechanism for both the superconductor(S)/normal metal(N) and S/S′ multilayers[12,13] and found that the behavior of $F_{p\perp max}$ as a function of λ and the size of the pinning are very similar for both systems despite that one has S intervening layer and another has N intervening layer.

In S/N multilayers the transverse pinning force $F_{p\perp}$ is usually much enhanced compared to the longitudinal pinning force $F_{p\parallel}$. In S/N multilayers the N layer usually works as an attractive pin center for vortices. So the fluxoids are stabilized in N sublayers. In this case the superconducting condensation energy is the main origin of the vortex pinning energy. In contrast, in the S/S′ multilayers such as NbTi/Nb, which has almost the same condensation energy between S and S′ layers, the main origin of the transverse pinning force may come from the kinetic term of the GL free energy.[14] This energy term stabilizes the fluxoids in NbTi sublayers as suggested by Matsushita *et al.*[15,16] In this case, Nb-layer works as the repulsive pin center. They demonstrated that in S/S′ multilayer ($\xi_s < \xi_{s'}$, where

ξ_s and $\xi_{s'}$ are the GL-coherence length of S and S′ layer, respectively), the large enhancement occurs in F_p, where S′ layer works as a repulsive pinning center.

We have investigated the $F_{p\perp}$ in three series of Nb_xTi_{100-x}/Nb (with $x = 65$, 50 and 28) and $Nb_{28}Ti_{72}/Nb_{65}Ti_{35}$ (S/S′) multilayers. We discuss about the maximum value of $F_{p\perp max}$ versus λ curve as a function of the difference of the coherence length of both the sublayer.

2. EXPERIMENTAL

Superconductor(S)/ superconductor(S′) multilayers have been fabricated by an RF dual sputtering onto quartz substrates. Samples are composed of three series of NbTi/Nb ($Nb_{65}Ti_{35}$/Nb, $Nb_{50}Ti_{50}$/Nb and $Nb_{28}Ti_{72}$/Nb) and one series of NbTi/NbTi ($Nb_{28}Ti_{72}/Nb_{65}Ti_{35}$). Samples thus made are designed to have equal sublayer thickness, $d_{NbTi} = d_{Nb}$ (or $d_{NbTi}) = (1/2)\lambda$, where d_{NbTi} and d_{Nb} mean the thickness of the NbTi-layer and Nb-layer, respectively, and λ is the modulation wavelength. The sample thickness is about 500 nm. The critical current density was measured resistively at 4.2 and 1.5 K under the magnetic field parallel to the layer plane ($J_c(H_\parallel)$) and perpendicular to the layer plane ($J_c(H_\perp)$), where $H_\parallel$ and $H_\perp$ are applied fields parallel and perpendicular to the layer, respectively. The macroscopic transverse and longitudinal pinning forces $F_{p\perp}$ and $F_{p\parallel}$ were calculated from the critical current density J_c as $F_{p\perp} = (1/c)J_c(H_\parallel) \times H_\parallel$ and $F_{p\parallel} = (1/c)J_c(H_\perp) \times H_\perp$. The schematic configurations for these quantities J, H and F are illustrated in Fig. 1.

3. RESULTS AND DISCUSSION

The field dependence of critical current densities $J_c(H_\parallel)$ and $J_c(H_\perp)$ at 1.5 K are shown in Fig. 2 a and b for $Nb_{50}Ti_{50}$/Nb-samples as a typical

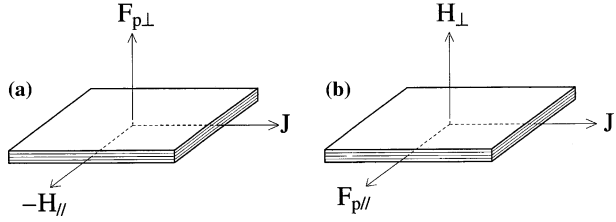

Fig. 1. Schematic configuration expressing the relation among *J, H* and *F* for both the cases of (a) *H* being parallel to the layer plane, and (b) *H* being perpendicular to the layer plane. J is always in the layer plane.

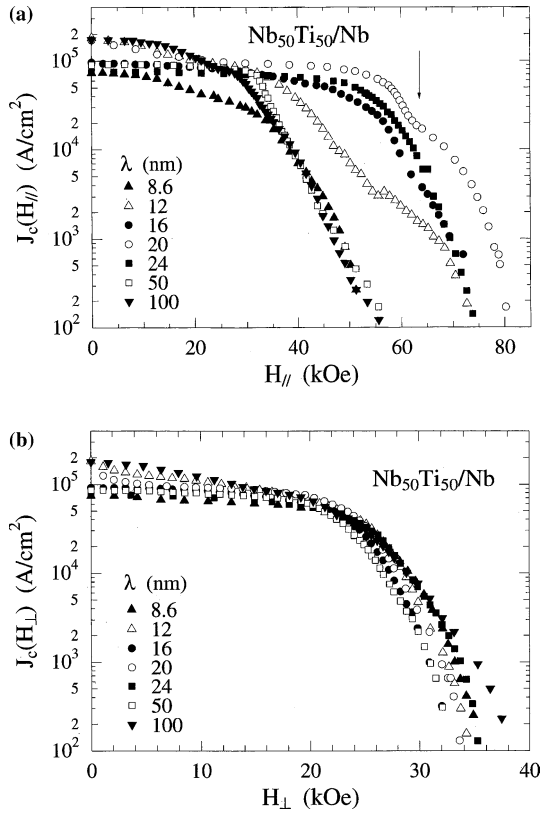

Fig. 2. Critical current density J_c under (a) the parallel magnetic field $H_\parallel$ and (b) the perpendicular magnetic field $H_\perp$ at 1.5 K for $Nb_{50}Ti_{50}$/Nb samples with changing of λ from 8.6 to 100 nm. An arrow in Fig. 2a indicates the jumping point of the vortex for the sample with $\lambda = 20$ nm (see the text).

example. The macroscopic transverse pinning force $F_{p\perp}$ as a function of $H_\parallel$ and longitudinal pinning force $F_{p\parallel}$ as a function of $H_\perp$ for the same samples are shown in Fig. 3a and b, respectively. From these figures we can see several characteristic features: (i) For small $\lambda(\lambda = 8.6\,\text{nm})$ and large $\lambda(\lambda = 100\,\text{nm})$ the pinning force $F_{p\perp}$ is relatively small because the layer itself or layer boundary does not work effectively as a pinning center and also because of the relatively small upper critical field $H_{c2\parallel}$.[17] Consequently, the peak of the pinning force $F_{p\perp max}$ is also small. (ii) In the quasi-2D region ($\lambda \sim 20\,\text{nm}$) the pinning force $F_{p\perp}$ is much enhanced which may be due to the Nb layer acting as the repulsive pinning center as discussed later. (iii) $F_{p\parallel}$ scarcely depends on λ because in the layer plane

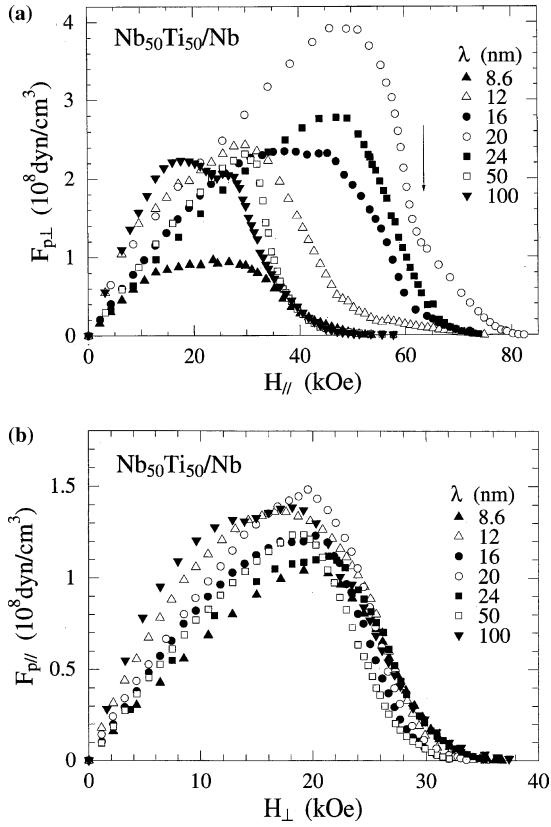

Fig. 3. (a) Pinning force $F_{p\perp}$ of the same series as Fig. 2 under the parallel magnetic field $H_{\parallel}$ and (b) $F_{p\parallel}$ under the perpendicular magnetic field $H_{\perp}$ at 1.5 K, which are calculated from J_c using the relations, $F_{p\perp} = (1/c) J_c(H_{\parallel}) \times H_{\parallel}$ and $F_{p\parallel} = (1/c) J_c(H_{\perp}) \times H_{\perp}$. An arrow in Fig. 3a indicates the vortex jumping point for the sample with $\lambda = 20$ nm.

direction there is no special pinning center which depends on the intervening layer thickness.

From the curve of F_p versus H, we can estimate the maximum value of the pinning force F_{pmax} for each sample with different λ. Both of thus obtained $F_{p\perp max}$ and $F_{p\parallel max}$ as a function of λ are illustrated in Fig. 4 for the present multilayers $Nb_{65}Ti_{35}$/Nb, $Nb_{50}Ti_{50}$/Nb, $Nb_{28}Ti_{72}$/Nb and $Nb_{28}Ti_{72}$/$Nb_{65}Ti_{35}$. The characteristic results are as follows: (i) The values of $F_{p\perp max}$ is about $1 \sim 7 \times 10^8$ dyn/cm^3 for all the present multilayers. This value is nearly the same order of magnitude as that of commercial NbTi alloy. (ii) For all series, $F_{p\perp max}$ is always larger than $F_{p\parallel max}$ except

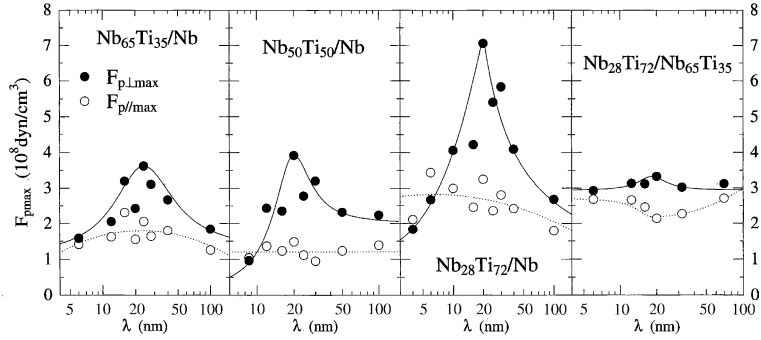

Fig. 4. Maximum pinning force $F_{p\perp max}$ and $F_{p\parallel max}$ as a function of λ at 1.5 K for the present multilayer series, $Nb_{65}Ti_{35}$/Nb, $Nb_{50}Ti_{50}$/Nb, $Nb_{28}Ti_{72}$/Nb and $Nb_{28}Ti_{72}/Nb_{65}Ti_{35}$. Lines are guide to the eyes.

for the smallest λ region. (iii) $F_{p\parallel max}$ is almost invariable over the entire λ range for all the multilayers investigated, suggesting that the pinning force acting parallel to the layer plane does not depend on the sublayer thickness, that is, in the direction of layer plane there exists no special pin center which depends on the layer thickness. It is quite reasonable because the pinning force acting parallel to the layer plane may be in the same situation to the case of $F_{p\parallel}$ in a single layer. (iv) $F_{p\perp max}$ as a function of λ has broad maximum around $\lambda \sim 20$ nm for all the present multilayer series. Therefore $F_{p\perp max}$ is strongly enhanced in this region.

The scattering of the $F_{p\parallel}$ values between sample to sample in the same series and/or between series seen in this figure may come from the difference in local pin centers formed by for example void, precipitation or dislocation. These local pins may influence equivalently both the transverse and longitudinal directions. Therefore, in order to evaluate more precisely the pinning force due to the pure effect of multilayering, the better method is to take the difference between. $F_{p\perp max}$ and $F_{p\parallel max}$ for each sample. We introduce here the effective pinning force F_{pLmax}. The value of $F_{pLmax} \equiv F_{p\perp max} - F_{p\parallel max}$. F_{pLmax} as a function of λ for all the series is shown in Fig. 5. In this figure the negative values of F_{pLmax} seen in the small λ region of $Nb_{28}Ti_{72}$/Nb and $Nb_{50}Ti_{50}$/Nb are due to the larger longitudinal pinning compared to the transverse pinning. As the multilayering is not effective in this region, the negative values have no important meaning. Here we can see the effect of layering on the pinning force for all the series. The large enhancement is also seen around $\lambda \sim 20$ nm for all the multilayer series which is in the quasi-2D region for the superconductivity. The peak value ($M(F)$) of the F_{pLmax} versus λ curve is the largest

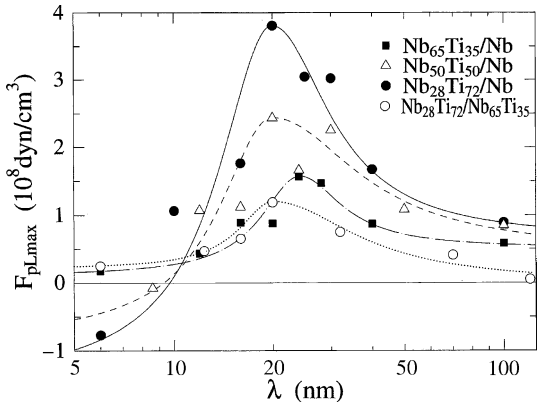

Fig. 5. Effective pinning force $F_{pLmax}(\equiv F_{p\perp max} - F_{p\parallel max})$ due to multilayering as a function of λ at 1.5 K. Lines are guide to the eyes.

for Nb_{28} Ti_{72}/Nb. The difference of $M(F)$ among the series is expected to originate from the difference in GL-coherence length ξ_{GL} of S′ layer and S layer.

According to the measurement of parallel and perpendicular upper critical field,[17,18] the GL-coherence length$\xi_{GL}(0)$ of sputtered Nb, $Nb_{65}Ti_{35}$, $Nb_{50}Ti_{50}$ and $Nb_{28}Ti_{72}$ at 0 K is estimated as 10.00, 6.34, 5.89 and 4.24 nm, respectively. The result of $\xi_{GL}(0)$ is shown in Fig. 6. The $\xi_{GL}(0)$ values have nearly a linear relation with respect to the Ti-concentration, suggesting that alloy-layer becomes dirtier by the substitution of Nb by Ti.

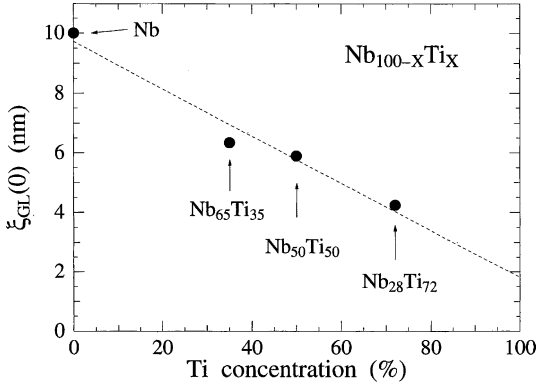

Fig. 6. GL-coherence length at 0K $\xi_{GL}(0)$ versus Ti-concentration for the Nb and NbTi alloy sublayers.

We now consider about the large enhancement of F_{pLmax} around $\lambda \sim 20\,\mathrm{nm}$ as seen in Fig. 5. In this region, as mentioned above, the superconducting state is quasi-2D as indicated by the dimensional crossover in $H_{\mathrm{c2}\parallel}$.[17,18] Therefore the quasi-2D state is related to the large enhancement of F_{pLmax}. One reason of the large enhancement is that the size of vortex just matches to the sublayer thickness in this region and consequently the vortex is hard to move even under the applied high magnetic field and/or the large current. Another reason of large enhancement is as follows. The phenomenon of the large enhancement of $F_{\mathrm{p}\perp}$ at the quasi-2D state in the S/S′ multilayers is similar to that of S/N multilayers.[13] Moreover the size of $F_{\mathrm{p}\perp\mathrm{max}}$ is nearly the same for both multilayer systems. S/N multilayer such as NbTi/Ti has pin center in the normal Ti-layer, which acts as attractive pin. The same situation is anticipated in the S/S′ multilayer such as NbTi/Nb. In this case Nb-layer, which has larger coherence length than NbTi layer, is considered to work as a repulsive pin,[15,16] signifying that the vortices preferably occupy the NbTi layer. This situation is realized as follows. In the quasi-2D region of S/S′ multilayer with different electron diffusion constant between S and S′, the two stage crossover occurs in the $H_{\mathrm{c2}\parallel}$ versus T curve as predicted theoretically by Tachiki and Takahashi.[3,4] Near T_{c}, $H_{\mathrm{c2}\parallel} - T$ curve behaves as anisotropic three dimension (3D), where the superconducting order parameter spreads over both the S and S′ layers. With decreasing temperature, $H_{\mathrm{c2}\parallel} - T$ curve upturns accompanying a kink at a certain temperature $T = T^{+}$ and the system behaves as two dimensional ($2\mathrm{D}^{+}$ state), where the superconducting order parameter locates in Nb layer (having a longer coherence length) and vortex is mainly located in NbTi layer. With further decreasing T, $H_{\mathrm{c2}\parallel} - T$ curve upturns again at another temperature $T = T^{*}$ and system enters into another two dimensional state (2D* state). The order parameter then is located in NbTi layer (having a shorter coherence length) near $H_{\mathrm{c2}\parallel}(T)$ and vortices moves to the Nb layer from NbTi layer with decreasing temperature. A typical example is shown in Fig. 7a for the case of $\mathrm{Nb_{65}Ti_{35}/Nb}(\lambda = 20\,\mathrm{nm})$. In this sample, as T^{+} is very close to T_c the upturn of $H_{c2\parallel}$ at T^{+} is not apparently visible in the figure. T^{*} can be identified at about 6 K as a kink of the $H_{c2\parallel}(T)$ curve. If we assume that the order parameter persists in the Nb layer over the entire temperature range below T_{c}, the hypothetical upper critical field $H^{*}(T)$ is expected to follow the dotted line in Fig. 7a.[18] Figure 7b presents the J_{c} versus $H_{\parallel}$ curves at 1.5 and 4.2 K for $\mathrm{Nb_{65}Ti_{35}/Nb}$ ($\lambda = 20\,\mathrm{nm}$). The J_{c} ($H_{\parallel}$) has a kink around 50 kOe at 1.5 K and around 30 kOe at 4.2 K. It is quite interesting to note that 50 kOe corresponds to $H^{*}(1.5\,\mathrm{K})$ and 30 kOe corresponds to $H^{*}(4.2\,\mathrm{K})$ in Fig. 7a. These kinks indicate the jump

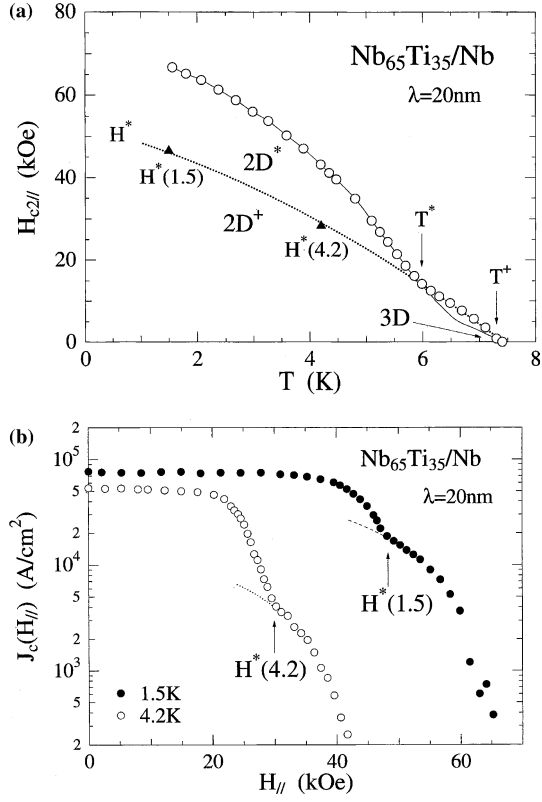

Fig. 7. (a) H–T diagram of $Nb_{65}Ti_{35}$/Nb for $\lambda = 20$ nm sample: circle: $H_{c2\|}$ data, triangle: transition field at 4.2 and 1.5 K from the measurement of $J_c(H_\|)$. Solid line and dotted line show $H_{c2\|}$ curves when order parameter is located in S′-sublayer (NbTi) and S-sublayer (Nb). T^+, T^* and, H^* are the transition temperature and transition field. 3D, $2D^+$ and 2D* are the corresponding superconducting states. (b) J_c versus $H_\|$ curve at 1.5 and 4.2 K of $Nb_{65}Ti_{35}$/Nb for $\lambda = 20$ nm sample. Kink appearing for each curve at $H^*(1.5)$ and $H^*(4.2)$ (arrow indicated) corresponds to the transitions from $2D^+$ to 2D* state.

of the order parameter from the Nb-sublayer (low field side) to the NbTi-sublayer (higher field side). This phenomenon clearly occurs when the size of vortex ($\sim \xi$) becomes comparable to the sublayer thickness. The vortices arrangement at the $2D^+$-state and 2D*-state is schematically drawn in Fig. 8. As shown in this figure, in the $H < H^*$ region ($2D^+$-state) vortices are located in the NbTi-layer while in the $H > H^*$ region (2D*-state) they are located in the Nb-layer. Therefore if the Nb-layer (having larger coherence length) works as the repulsive pin center, $2D^+$ state has larger pinning force than 2D* state. This situation is substantiated by the behavior

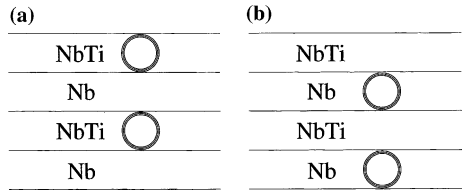

Fig. 8. Vortices arrangement at (a) the $2D^{+}$-state and (b) the 2D*-state.

of the $J_c(H_\parallel)$-curve as shown in Fig. 7b, where the large enhancement of $J_c(H_\parallel)$ is observable at field below H^*. The $J_c(H_\parallel)$ kink and the enhancement of $F_{p\perp}$ at the boundary between $2D^{+}$ and 2D* can be also seen for other series, for example in $Nb_{50}Ti_{50}$/Nb-sample of $\lambda = 20\,\text{nm}$ in Figs. 2a and 3a (marked by an arrow). Thus the kink of the $J_c(H_\parallel)$ at H^* provides a direct evidence of the repulsive pinning due to the Nb-layer.

Mechanism of repulsive pinning has been first treated for the longitudinal pin by Matsushita *et al.*[16] for NbTi/Nb lamella structure. They have deduced the elementary pinning force $f_{p\parallel}$ (see Eq. 11 of Ref. 16) acting on the longitudinal direction to the layer plane based on the Ginzburg–Landau theory. The repulsive pinning force comes from the kinetic energy difference between the both layers due to the spatial variation of the order parameter. Based on their theory we have calculated the transverse pinning force for the present S/S′ multilayers. The free energy in the superconducting state F_s is written down as follows.

$$F_s = F_n(0) + \alpha|\Psi|^2 + \frac{\beta}{2}|\Psi|^4 + \frac{1}{2m^*}|(-i\hbar\nabla + 2e\mathbf{A})\Psi|^2 + \frac{1}{2}\mu_0(\text{rot}\mathbf{A})^2, \quad (1)$$

where $F_n(0)$ is the free energy in the normal state in the absence of magnetic field, Ψ the order parameter, m* the mass of superconducting electron, μ_0 the permeability of vacuum, $\boldsymbol{A}$ the vector potential, and α and β are the numerical coefficients. In the NbTi/Nb, T_c of both the layers is nearly the same and the density of state is also comparable.[17,19] The vortex pinning is mainly correlated to the change of kinetic and potential energy caused by the spatial variation of the order parameter. Here we can put $\Delta\Psi = |\Psi|/|\Psi_\infty| = 3r/2a_0 - r^3/2a_0^3$ $(r \leqslant a_0)$ and $\Delta\Psi = 1 (r > a_0)$ around a fluxoid,[20] where Ψ_∞ is the equilibrium value of order parameter and r the position within the fluxoid, $r = 0$ is the position of the center of the fluxoid core and $a_0 = (8/3)^{1/2}\xi$. The increase of the energy E_1 by having the fluxoid in the layer is;[21]

$$E_1 = \int_0^{a_0} \left[\alpha|\Psi|^2 + \frac{\beta}{2}|\Psi|^4 + \frac{\hbar}{2m^*}\left(\frac{\partial|\Psi|}{\partial r}\right)^2 \right] 2\pi r\, dr$$

$$-\pi a_0\left(\alpha|\Psi_\infty|^2+\frac{\beta}{2}|\Psi_\infty|^4\right)$$
$$\sim \pi\mu_0 H_c^2\xi^2. \tag{2}$$

At the boundary region between NbTi-layer and Nb-layer, a_0 must be taken as the average value of both the coherence lengths as $a_0 = (8/3)^{1/2}(\xi_{NT}+\xi_N)/2$, where ξ_N and ξ_{NT} are the GL-coherence length of Nb and NbTi layer, respectively. The elementary pin $f_{p\perp}$ working at the boundary of both layers NbTi and Nb acting on the perpendicular direction to the layer plane is thus,

$$f_{p\perp} = \frac{\partial \Delta E_1}{\partial r} = \frac{E_{1N}-E_{1NT}}{2a_0} = \frac{\pi\mu_0 H_{cN}^2\xi_N^2 - \pi\mu_0 H_{cNT}^2\xi_{NT}^2}{2(8/3)^{1/2}(\xi_{NT}+\xi_N)/2}$$
$$\sim (3/8)^{1/2}\pi\mu_0 H_c^2(\xi_N-\xi_{NT}), \tag{3}$$

where suffix N and NT mean Nb and NbTi layer, respectively. Here we assume that the thermodynamical critical field H_c for both NbTi and Nb layer are almost same as $H_c \sim H_{cNT} \sim H_{cN}$. Usually the macroscopic pinning force is written as $F_p \sim \varepsilon N f_p$,[22] where ε is the efficiency factor of pin and N the effective pin density. Therefore F_{pLmax} is regarded to be proportional to $f_{p\perp max}$ as $F_{pLmax} \propto f_{p\perp}$. So, from the Eq. (3) we can conclude that if the pinning force originates from the repulsive pin, the relation $F_{pLmax} \propto \xi_N - \xi_{NT}$ must hold for the multilayers systems.

We plot the values of $M(F)$ as a function of $\xi_N - \xi_{NT}$ at 1.5 and 4.2 K shown in Fig. 9, where the values listed in Fig. 6 are taken for ξ_N and ξ_{NT}. In this figure we can see that $M(F)$ and $\xi_N - \xi_{NT}$ have a roughly

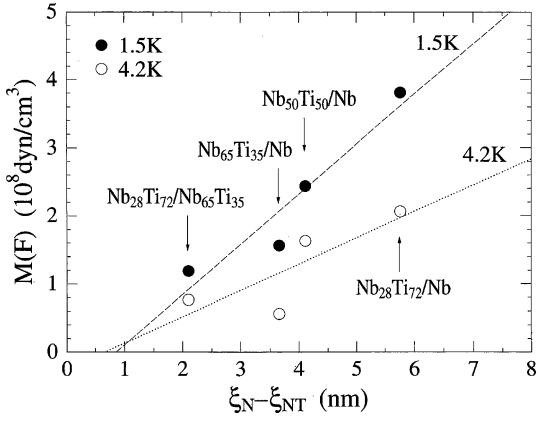

Fig. 9. Peak of maximum, pinning force $M(F)$ versus $\xi_N - -\xi_{NT}$ for the present multilayer series at 1.5 and 4.2 K.

linear relation. Thus in the present S/S′ multilayers, the repulsive pinning force actually acts on the systems as the main pin, the strength of which is of the same order as the usual attractive pinning force.

4. SUMMARY

The superconductor/superconductor multilayer NbTi/Nb has the large enhanced transverse pinning force $F_{p\perp max}$ compared to the longitudinal pinning force $F_{p\parallel max}$. This large $F_{p\perp max}$ is comparable to that of superconductor/normal metal multilayer NbTi/Ti. Present series of Nb_xTi_{100-x}/Nb with $x=65$, 50 and 28 and $Nb_{28}Ti_{72}/Nb_{65}Ti_{35}$ show the broad peak in the F_{pLmax} (the effective pinning force due to multilayering) versus λ at the quasi-2D region. The peak value of F_{pLmax} ($M(F)$) as a function of $\xi_N - \xi_{NT}$ satisfies nearly a linear relation. This should originate from the superconducting Nb layers acting as repulsive pin centers. With increasing $H_\parallel$, the vortices jump from the NbTi sublayer to the Nb sublayer at $H^*(T)$ because of the repulsive pinning force, $H^*(T)$ being the extrapolated hypothetical $H_{c2\parallel}$ (T) of the $2D^{3+}$ state of the superconductor/superconductor multilayer where the order parameter is fixed in the Nb sublayer.

REFERENCES

1. M. Tinkham, *Introduction to Superconductivity*, McGraw-Hill, Inc. Press, New York, USA (1975).
2. S. Takahashi and M. Tachiki, *Phys. Rev. B* **33**, 4620 (1986).
3. S. Takahashi and M. Tachiki, *Phys. Rev. B* **34**, 3162 (1986).
4. M. Tachiki and S. Takahashi, *Physica B* **169**, 121 (1991).
5. S. Takahashi, T. Hirai, and M. Tachiki, *Proc. SPIE-Int. Soc. Opt. Eng.* (USA), **2157** 263 (1994)
6. M. Tachiki and S. Takahashi, *Solid State Commun.* **70**, 291 (1989).
7. H. Raffy and J. C. Renard, *Solid State Commun.* **11**, 1679 (1972).
8. P. R. Brossard and T. H. Geballe, *Phys. Rev. B* **37**, 68 (1988).
9. Y. Obi, M. Ikebe and H. Fujimori, *Jpn. J. Appl. Phys.* **31**, 1334 (1992).
10. M. Ikebe, Y. Obi, H. Fujishiro, and H. Fujimori, *Jpn. J. Appl. Phys.* **32**, 55 (1993).
11. Y. Obi, M. Ikebe, Y. Muto, and H. Fujimori, *Trans. JIM* **29**, 313 (1988).
12. M. Ikebe, Y. Obi, H. Fujishiro, and H. Fujimori, *Czech. J. Phys.* **46 Suppl. S2**, 719 (1996).
13. Y. Obi, H. Fujimori, M. Ikebe, and H. Fujishiro, *Superlattice. Microst.* **21**, 423 (1997).
14. Y. Obi, M. Ikebe, H. Fujishiro, and H. Fujimori, *Physica B* **284–288** 857 (2000).
15. K. Matsumoto, H. Takewaki, Y. Tanaka, O. Miura, K. Yamafuji, K. Funaki, M. Iwakuma, and T. Matsushita, *Appl. Phys. Lett.* **64** 115 (1994).
16. T. Matsushita, M. Iwakuma, K. Funaki, K. Yamafuji, K. Matsumoto, O. Miura, and Y. Tanaka, *Adv. Cryog. Eng.* **42** 1103 (1996).
17. Y. Obi, S. Takahashi, H. Fujimori, M. Ikebe, and H. Fujishiro, *J. Low Temp. Phys.* **96** 1 (1994).
18. Y. Obi, M. Ikebe, H. Fujishiro, K. Takanaka, and H. Fujimori, *Phys. Stat. Sol. (b)* **223** 799 (2001).
19. Y. Obi, M. Ikebe, and H. Fujimori, *J. Phys. Soc. Jpn.* **66** 3600 (1997).

20. T. Matsushita, *Magnetic Flux Pinning and Electromagnetic Phenomena*, Sangyo-tosho, Tokyo, Japan, p. 236 (1994).
21. This equation has nearly the same meaning as the Eq. 1 of Ref. 15 by Matsushita *et al.*
22. W. A. Fietz and W. W. Webb, *Phys Rev*. **178** 657 (1969).